Research Square

Preprints are preliminary reports that have not undergone peer review.
They should not be considered conclusive, used to inform clinical practice,
or referenced by the media as validated information.

Ws-Gdm Framework: Integrating Adaptive Waypoint Generation with Classical Path Sequencing for Gas Distribution Mapping in Unknown Environment

MUQRI MUAZAM ZAINAL

muqrimuazam@studentmail.unimap.edu.my

Universiti Malaysia Perlis

KAMARULZAMAN KAMARUDIN

Universiti Malaysia Perlis

NASR ABDALMANAN

Universiti Malaysia Perlis

WAN RAHIMAN WAN ABDUL AZIZ

Universiti Sains Malaysia

M AIZAT ABU BAKAR

Universiti Malaysia Perlis

Research Article

Keywords: Gas Distribution Mapping, Path Planning, Waypoint Sequencing, Mobile Robot, Environmental Monitoring

Posted Date: November 23rd, 2026

DOI: https://doi.org/10.21203/rs.3.rs-8291815/v1

License: This work is licensed under a Creative Commons Attribution 4.0 International License.
Read Full License

Additional Declarations: No competing interests reported.

WS-GDM FRAMEWORK: INTEGRATING ADAPTIVE WAYPOINT GENERATION WITH CLASSICAL PATH SEQUENCING FOR GAS DISTRIBUTION MAPPING IN UNKNOWN ENVIRONMENT

Author Information:

1. Muqri Muazam Zainal (Mechatronic Department, Faculty of Electrical Engineering & Technology, Universiti Malaysia Perlis, 02600 Arau, Perlis) (muqrimuazam@gmail.com) (0009-0005-3070-3342) *(Corresponding Author)*

2. Kamarulzaman Kamarudin (Mechatronic Department, Faculty of Electrical Engineering & Technology, Universiti Malaysia Perlis, 02600 Arau, Perlis) (kamarulzaman@unimap.edu.my) (0000-0001-7764-0821) *(Corresponding Author)*

3. Nasr Abdalmanan (Mechatronic Department, Faculty of Electrical Engineering & Technology, Universiti Malaysia Perlis, 02600 Arau, Perlis) (nasr@studentmail.unimap.edu.my) (0000-0002-6366-626X)

4. Wan Rahiman Wan Abdul Aziz (School of Electrical and Electronic Engineering, Universiti Sains Malaysia, Pulau Pinang, Malaysia) (wanrahiman@usm.my) (0000-0003-1662-7484)

5. M Aizat Abu Bakar (Mechatronic Department, Faculty of Electrical Engineering & Technology, Universiti Malaysia Perlis, 02600 Arau, Perlis) (aizatbakar@unimap.edu.my) (0000-0002-4011-0787)

ABSTRACT

Gas distribution mapping is a critical task for mobile robots in environmental monitoring applications, where path planning strategies significantly influence both exploration efficiency and mapping accuracy. However, existing approaches often optimize path efficiency and mapping quality independently, lacking integrated frameworks that systematically combine adaptive waypoint generation with path sequencing optimization while considering their joint impact on mapping quality. Moreover, existing studies typically assume known environments or predefined exploration paths, overlooking gas distribution mapping scenarios where both the spatial structure and gas distribution are completely unknown to the robot. To address this challenge, this paper proposes the Waypoint-Sequencing Gas Distribution Mapping (WS-GDM) Framework, a comprehensive system consisting of three integrated components including adaptive Gaussian K-Means clustering for waypoint generation, a classical path sequencing algorithm for trajectory planning, and Kernel DM+V for gas field reconstruction. The framework operates in completely unknown environments, simultaneously discovering spatial structure and gas distribution through adaptive exploration. To validate the framework and identify the optimal path sequencing algorithm, WS-GDM was tested with four classical methods including Nearest Neighbour (NN), TSP with Nearest Neighbour initialization (TSP-NN), NN with 2-opt optimization (NN-2opt), and Ant Colony Optimization (ACO). Each variant was evaluated in simulated indoor environments across coverage completeness, path efficiency, completion time, gas mapping accuracy, and source localization precision. Results demonstrate that WS-GDM with NN-2opt achieved the best overall performance with highest area coverage at 85.54% and most accurate source localization at 0.524m average error, significantly outperforming NN, TSP-NN, and ACO, with ACO showing 110.88% higher localization error. Based on comprehensive evaluation, WS-GDM with NN-2opt demonstrates the best balance between operational efficiency and mapping accuracy, making it the recommended configuration for autonomous gas distribution mapping application.

Keyword: *Gas Distribution Mapping, Path Planning, Waypoint Sequencing, Mobile Robot, Environmental Monitoring*

1.0 INTRODUCTION

Autonomous mobile robots have become essential tools in a variety of real-world applications such as environmental monitoring, industrial inspection, and disaster response, including gas leak source detection[1]. One of the key capabilities that enables mobile robots to execute various types of navigation tasks is path planning, which computes the route and trajectory for the robot to visit designated locations in a specified environment [2]. In particular, mobile robots with path planning capabilities that are involved in data collection tasks such as detecting gas leak sources and mapping gas readings may require visiting multiple points, which significantly influences both exploration efficiency and mapping accuracy [3]. Therefore, developing an integrated framework that systematically combines waypoint generation with path sequencing to ensure full coverage of all sampling points while minimizing travel cost and maximizing sensing quality remains a critical and ongoing research challenge.

While recent advances in machine learning, particularly reinforcement learning, have shown promise in path planning, this paper focuses on traditional optimization methods for gas distribution mapping, which remain widely applicable and computationally efficient in resource-constrained robotic systems. Traditional path planning algorithms can generally be divided into two categories including reactive navigation and coverage-based planning [4], [5], [6]. Reactive navigation focuses on reaching a goal while avoiding obstacles, relying primarily on local information and greedy decision-making methods such as the Nearest Neighbour (NN) approach. These methods are computationally efficient and simple to implement but often fail to guarantee full coverage, potentially missing sampling points or regions due to its localized decision-making [7]. In contrast, coverage-based planning aims to ensure systematic exploration of all regions, typically employing sweeping patterns or grid-based spatial decomposition [8]. However, these methods can become computationally inefficient as the number of sampling points increases, particularly in scenarios requiring high spatial resolution mapping, such as gas distribution modelling.

To address the limitations of purely reactive or coverage-based methods, the Travelling Salesman Problem (TSP) offers a mathematically rigorous framework for optimizing visiting sequences among multiple target points. In the context of mobile robotics, solving the TSP ensures that all target locations are visited exactly once while minimizing total travel distance, thereby balancing coverage completeness with path efficiency [9], [10], [11]. However, solving the classical TSP optimally is a complex task, particularly in dynamic environments or when the number of sampling points is large. Consequently, heuristic and metaheuristic algorithms such as the Nearest Neighbour heuristic, 2-opt local search, and Ant Colony Optimization (ACO) have been widely adopted to generate near-optimal solutions [12], [13], [14], [15]. Among these approaches, 2-opt and ACO are particularly promising due to each method effectiveness in iterative path refinement and adaptive route optimization, respectively.

Despite the widespread application of TSP-based methods for efficient route planning, existing gas distribution mapping approaches often treat waypoint generation and path sequencing as separate processes, lacking optimized frameworks that systematically integrate adaptive waypoint generation with path sequencing while examining their combined effect on mapping quality. Most existing studies focus primarily on minimizing travel distance or improving exploration speed but rarely examine how different path sequencing strategies affect the quality of the resulting gas distribution map [16], [17], [18]. Specifically, while existing works optimize path efficiency independently of sensing performance, the impact of waypoint visiting sequences on gas map reconstruction accuracy and source localization precision within a unified framework has not been systematically investigated. This gap creates a need for an integrated system that combines adaptive waypoint generation with classical path sequencing

methods while providing empirical guidance on selecting the most appropriate sequencing algorithm for gas distribution mapping applications.

To address this gap, this paper proposes the Waypoint-Sequencing Gas Distribution Mapping (WS-GDM) Framework, an integrated system that combines adaptive waypoint generation with classical path sequencing methods for efficient and accurate gas distribution mapping. The framework consists of three main components including adaptive Gaussian K-Means clustering for intelligent waypoint generation based on predicted gas distribution, a path sequencing module employing classical TSP-based algorithms, and Kernel Density Estimation with Variance (Kernel DM+V) for probabilistic gas field reconstruction. A critical aspect of framework development is selecting an appropriate path sequencing algorithm, as different classical methods may produce varying impacts on both operational efficiency and mapping quality. To identify the optimal sequencing method for the WS-GDM framework, this study conducts a systematic comparative evaluation of four classical path sequencing strategies including Nearest Neighbour (NN), TSP with Nearest Neighbour initialization (TSP-NN), NN with 2-opt optimization (NN-2opt), and Ant Colony Optimization (ACO) implemented within the proposed framework under controlled simulation condition.

The main contributions of this work are:

- **WS-GDM Framework:** An integrated framework combining adaptive waypoint generation, classical path sequencing, and probabilistic gas field reconstruction for autonomous gas distribution mapping in unknown environments.
- **NN-2opt implementation for GDM**: Presents the first implementation and validation of Nearest Neighbour combined with 2-opt local search optimization as a path sequencing method specifically for gas distribution mapping applications.
- **Optimized Path Sequencing for GDM Exploration:** Systematic evaluation identifying NN-2opt as the optimal path sequencing method among four classical approaches (NN, TSP-NN, NN-2opt, ACO) within the WS-GDM framework, providing empirically validated guidance for autonomous gas distribution mapping.

The remainder of this paper is organized as follows: Section II reviews related work on classical path planning methods and gas distribution mapping approaches. Section III describes the WS-GDM framework architecture, methodology, and experimental setup, including the simulation environment and implementation details of each path sequencing variant. Section IV presents the comparative evaluation results of different WS-GDM configurations and discusses their implications for autonomous gas mapping. Finally, Section V concludes with the recommended WS-GDM configuration and outlines potential directions for future research.

2.0 RELATED WORK

- Path Planning for Multi-Goal Navigation

Recent studies have applied TSP-based methods and local search heuristics to optimize robot waypoint sequences. Kulich et al. formulated multi-goal exploration as the d-Watchman Route Problem and introduced IREANN, an evolutionary algorithm using extended nearest neighbour heuristics with priority lists to solve the Generalized TSP with Coverage constraints, achieving faster exploration in simulated and real environments [19]. Vonásek et al. developed Space-Filling Forest (SFF*), which grows multiple RRT trees simultaneously with priority queues biasing expansion toward nearby targets, producing shorter target-to-target paths and better TSP solutions than Multi-T-RRT and Lazy-TSP in obstacle-rich environments [20]. Yuanjie et al. integrated machine learning with TSP solvers by training

models to predict runtime and distance for single-goal problems, constructing cost matrices that enabled significantly faster multi-goal planning in cluttered environments with dynamic constraints [21].

Khumla et al. enhanced the 2-opt algorithm with a random shuffle mechanism (2-optRS) to escape local optima, achieving 7.3% shorter routes than traditional 2-opt for visiting 20 provinces in tested environment, though with increased computational time [22]. Banerjee et al. developed a Hybrid ACO-Two-opt approach for cold storage logistics in India, where ACO constructs initial tours through pheromone-guided exploration followed by 2-opt refinement, demonstrating superior route optimization and cost efficiency across 391 facilities and achieving near-optimal solutions on TSPLIB benchmarks [23].

Lu et al. combined improved ACO for global planning with Dynamic Window Algorithm for local obstacle avoidance, introducing adaptive pheromone initialization, ant colony division, deadlock detection, and path smoothing to achieve shorter paths and faster convergence in cluttered and maze-like environments [24]. Zhou et al. proposed four ACO enhancements including uneven pheromone initialization favouring goal proximity, adaptive volatility factors, reward-punishment update mechanisms, and path optimization which demonstrating shorter paths, faster convergence, and smoother trajectories across grid environments of increasing complexity [25].

While these approaches demonstrate that heuristic and metaheuristic methods including NN, ACO, and 2-opt can improve travel efficiency and scalability, each recent paper evaluations focus primarily on path length, computation time, and energy consumption. Critically, these studies do not assess how different visiting sequences affect sensing quality or the accuracy of collected environmental data, leaving the relationship between path order and mapping fidelity largely unexamined. Additionally, no existing work has explored the integration of NN with 2-opt optimization specifically for gas distribution mapping, despite the potential benefits of combining greedy initialization with local search refinement for environmental sensing tasks.

- Gas or environmental mapping with mobile robots

Recent advances in gas distribution mapping have increasingly adopted probabilistic and learning-based approaches. Gongora et al. developed Information-Driven Gas Distribution Mapping (IGDM), integrating the GW-GMRF real-time modelling algorithm with a POMDP planner that uses Kullback-Leibler Divergence-based rewards to guide multi-step exploration, demonstrating lower reconstruction error than randomized strategies in both simulation and wind tunnel experiments [26]. Kulbaka et al. proposed GDM-Net, a Deep Reinforcement Learning approach using offline Gaussian Process Regression to calculate reward functions based on posterior variance, enabling autonomous trajectory generation that outperformed random walk and greedy baselines across multiple gas types [27]. Winkler et al. introduced RABI-GNN, a Graph Neural Network using attention-based message passing to reconstruct 3D gas fields from irregularly sampled measurements, successfully generalizing from synthetic training data to real industrial environments [28].

Ercolani et al. developed Gas Simultaneous Localization and Mapping (GaSLAM), which simultaneously maps gas distribution and locates gas sources using adaptive navigation, outperforming separate approaches in wind tunnel experiments [29]. Waarum et al. addressed nonstationary in Gaussian Process models by introducing mixture modelling approaches (MoE, NLE, NLE-MA) that partition measurement space to capture different spatial statistics in emission plumes versus background regions, demonstrating effective representation of complex environmental fields in real UAV methane survey data [30].

In summary, two distinct research directions emerge which are TSP-based path optimization and probabilistic gas mapping. However, existing approaches typically optimize path efficiency and gas reconstruction separately, without an integrated framework that combines adaptive waypoint generation with path sequencing or examines their combined effect on sensing quality. Path planning research focuses on travel efficiency while gas mapping emphasizes reconstruction algorithms, leaving this integration unexplored. This separation creates a critical gap, as effective gas distribution mapping requires coordinated design of both components to maximize coverage and measurement accuracy. Moreover, existing studies typically assume either pre-mapped environments or predefined exploration trajectories. To the best of the authors' knowledge, no prior work has systematically evaluated classical path sequencing strategies for gas distribution mapping in completely unknown environments where both spatial structure and gas distribution must be discovered simultaneously through adaptive exploration. To address these gaps, this paper proposes the WS-GDM framework that adaptively explores unknown environments by integrating waypoint generation with classical path sequencing methods, identifying the optimal configuration through systematic evaluation.

3.0 METHODOLOGY

3.1 Overview and Conceptual of Proposed Framework

This section presents the Waypoint-Sequencing Gas Distribution Mapping (WS-GDM) Framework, an integrated system designed for autonomous gas distribution mapping. The framework consists of three main components including the Waypoint Generator, which identifies optimal sampling locations using adaptive Gaussian K-Means clustering based on predicted gas distribution. Then, the Path Sequencing Algorithm, which determines the visiting order of waypoints using classical TSP-based methods to optimize trajectory efficiency. The last component is Gas Distribution Mapping module, which reconstructs the concentration field from collected measurements using Kernel Density Estimation with Variance (Kernel DM+V) [31]. To identify the most effective path sequencing method for the framework, four classical algorithms are evaluated including Nearest Neighbour (NN), TSP with Nearest Neighbour initialization (TSP-NN), NN with 2-opt optimization (NN-2opt), and Ant Colony Optimization (ACO).

The WS-GDM framework operates through sequential integration of its three components, as illustrated in Fig. 1. The Waypoint Generator first analyses the environment and predicted gas distribution to produce a set of strategically positioned sampling coordinates. These coordinates are then passed to the Path Sequencing Algorithm, which computes an optimized visiting order based on the selected classical method. Following the computed sequence, the mobile robot navigates to each waypoint, collects gas concentration measurements, and performs real-time region extraction to identify potential new sampling locations. As the robot explores, the Waypoint Generator continuously analyses newly sensed regions and adaptively generates additional waypoints if unexplored areas with significant gas variations are detected [32]. These dynamically generated waypoints are incorporated into the visiting sequence, and the collected measurements are processed by the Gas Distribution Mapping module to progressively reconstruct the spatial concentration field. This integrated workflow ensures that waypoint selection, path optimization, and field reconstruction work cohesively to achieve efficient exploration and accurate environmental sensing. The framework is evaluated across multiple performance metrics including coverage completeness, path efficiency, completion time, gas mapping accuracy, and source localization precision to identify the optimal path sequencing configuration.

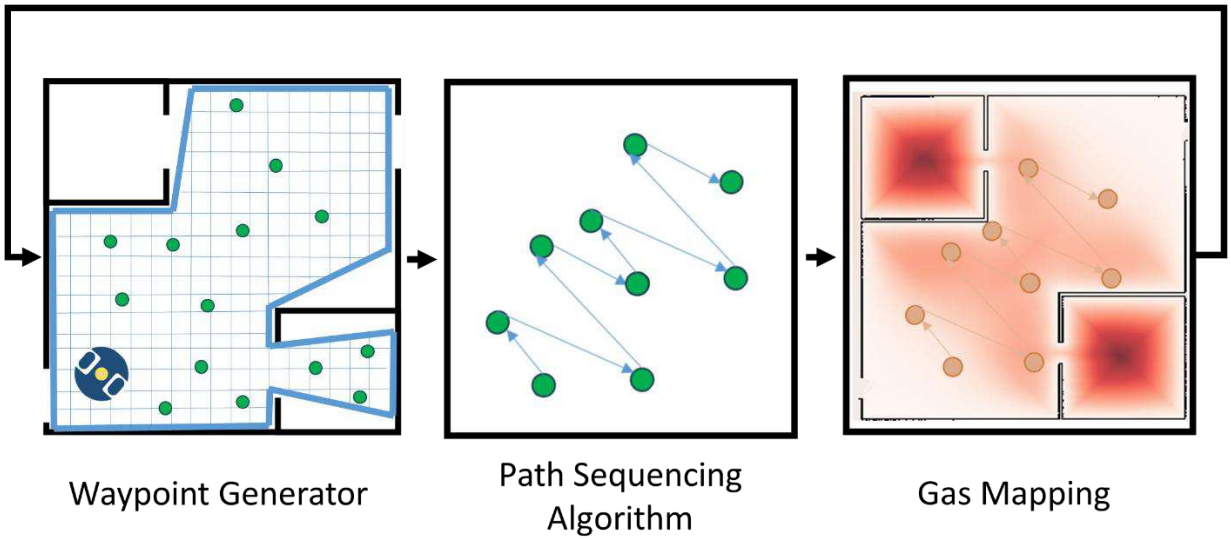

Fig 1. Path Planning Comparison Process Framework

3.2 Environment Setup

The simulation experiments were conducted in the ROS 2 and Gazebo environment to evaluate the relationship between path sequencing strategies and gas mapping performance under controlled conditions. The environment was modelled as a 10m × 10m indoor map, representing a typical operational space for mobile robot environmental exploration. The robot begins with no prior knowledge of either the environment structure or gas distribution, performing simultaneous localization, mapping, and gas sensing. As the robot explores, it builds an occupancy map using LiDAR-based mapping while simultaneously generating waypoints through adaptive clustering and collecting gas measurements. A differential drive mobile robot was used to navigate between designated waypoints at a constant velocity of 0.14 m/s. Rather than simulating physical gas sensors, a reference gas concentration map was pre-generated to serve as the ground truth distribution. During each simulation run, the robot's trajectory was recorded, and each waypoint visit was assigned a confidence value reflecting the degree of local area coverage. These confidence values were then mapped onto the reference distribution to reconstruct the perceived gas concentration field. This approach enables evaluation of path sequencing effects on mapping accuracy in realistic unknown environment scenarios while eliminating sensor-specific uncertainties for consistent and repeatable comparisons across all tested strategies.

Fig. 2 (left) shows the detailed dimensions and room layout, which was then constructed in Gazebo with identical dimensions as shown in Fig. 2 (right), including the red, green, and blue lines indicating the x, y, and z-axis of the simulation environment. The designated layout consists of a main entry, one main area, and two rooms positioned at the corners of the space. Each room has one entrance with identical dimensions. The main entry serves as the starting point for the mobile robot before it navigates to all designated waypoints. The mobile robot used in the simulator features a two-wheeled rear-drive configuration with one caster wheel for free motion. The primary sensor equipped on the mobile robot is a Light Detection and Ranging (LiDAR) sensor with a 12m maximum detection range.

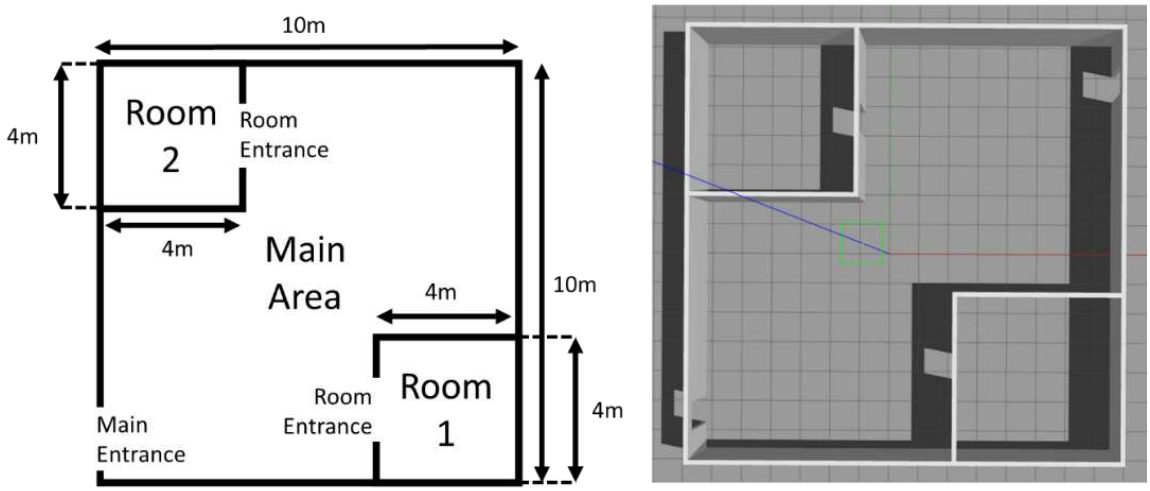

Fig 2. Dimension of Environment (Left) and Simulated Setup in Gazebo (Right)

The simulation was implemented using ROS 2 Humble and Gazebo Garden. Additional libraries included Simultaneous Localization and Mapping (SLAM) Toolbox for mapping coverage and Navigation 2 (Nav2) for autonomous waypoint navigation. All experiments were conducted on an Asus Vivobook Pro 15 laptop running Ubuntu 22.04, equipped with an AMD Ryzen 9 5900H processor (6 cores, 12 threads, 3.6GHz base frequency), 16GB RAM, 500GB SSD storage, and an Nvidia GeForce RTX 3050 graphics card with 6GB GDDR6 memory. These mid-to-high performance specifications ensured efficient simulation execution and reduced computational time.

3.3 Waypoint Generator Component

Following the simulation environment setup, the WS-GDM framework's Waypoint Generator component derives valid exploration regions from LiDAR measurements and determines representative sampling locations for autonomous navigation. This process employs a two-stage spatial processing approach including region extraction from LiDAR data to identify explorable areas, and density-aware Gaussian K-Means clustering for adaptive waypoint generation based on predicted gas distribution patterns.

3.3.1 Region Extraction from LiDAR Reading

Raw LiDAR scans provide a discrete set of points representing the boundaries of the observable environment. To define a continuous region suitable for spatial reasoning, these points are first projected into a two-dimensional coordinate set $\{(x_i, y_i)\}_{i=1}^{n}$. If the number of valid points $n \geq 3$, a polygonal boundary is constructed using the Shapely geometry library, represented as show in Equation (1)

$$\mathcal{P} = Polygon(\{(x_i, y_i)\}_{i=1}^{n}) \tag{1}$$

which describe the observable free space. The polygon bounds (x min, y min, x max, y max) are then computed to define the rectangular extent of the region. To discretize the interior of the polygon, a grid sampling process is performed according to the map resolution, denoted as Δr. The number of grid divisions along the x and y axes are computed as Equation (2).

$$N_x = \frac{x_{max} - x_{min}}{\Delta \mathrm{r}}, \qquad N_y = \frac{y_{max} - y_{min}}{\Delta \mathrm{r}} \tag{2}$$

Grid coordinates are generated for all (x, y) positions within these bounds using uniform spacing Δr. Only points satisfying the geometric inclusion condition $(x, y) \in \mathcal{P}$ are retained, ensuring that the generated grid points lie within the LiDAR-observed free space. This process yields a dense spatial representation of all feasible exploration positions that the robot can potentially visit.

3.3.2 Density-aware Gaussian K-Means Clustering for Waypoint Generation

The grid points obtained from the polygonal region are subsequently processed to identify representative waypoints that balance spatial coverage and computational efficiency. To achieve this, a density-aware Gaussian K-Means clustering method is introduced.

First, the Gaussian Kernel Density Estimation (KDE) is applied to the grid coordinates to infer the underlying spatial distribution of point density. The density function $\hat{f}(x)$ estimates the probability of spatial concentration, revealing areas of high environmental complexity or structural significance.

Next, a local density measure is computed using the Nearest Neighbours method, which counts the number of neighbouring points within a fixed radius r. The average local density $\overline{D}$ is then used to estimate the number of clusters k, ensuring adaptive adjustment to the density of the environment as shown in Equation (3).

$$k = max\left(1, \frac{N}{\overline{D}}\right) \tag{3}$$

where N is the total number of points within the region.

Using this estimated k, K-Means clustering partitions the spatial dataset into compact groups, with each cluster centroid representing an optimal waypoint. The centroid for each cluster C_j is computed using Equation (4):

$$C_j = \frac{1}{|S_j|} \sum_{x_i \in S_j} x_i \tag{4}$$

where S_j denotes the set of points assigned to cluster j.

This integrated process ensures that waypoint density corresponds directly to spatial complexity-denser in narrow or obstacle-rich regions and sparser in open spaces. Consequently, the resulting waypoints form a compact yet informative set that can be used for efficient robot exploration, mapping, and task execution.

The proposed approach automatically identifies meaningful waypoint distributions from real sensor data by combining LiDAR-based region extraction with adaptive Gaussian K-Means clustering. The method minimizes redundant navigation points while preserving environmental fidelity, making it particularly effective for autonomous tasks such as entrance detection, environmental mapping, or gas distribution exploration. Fig 3 illustrates the region extraction and waypoint generation process. First, the enclosed free-space region is extracted as a polygon based on the LiDAR scan data. The polygon is

discretized into points at 0.05 m spatial resolution. These points are then grouped using distance-based clustering, where each cluster represents an area of approximately 1 m in radius. The centroid of each cluster is selected as a waypoint.

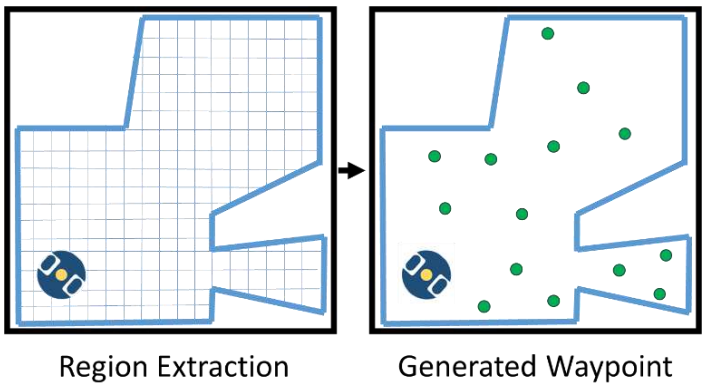

Fig 3. Region Extraction and Waypoint Generation Process

3.4 Path Sequencing Algorithm

After the Waypoint Generator produces optimal sampling locations, the WS-GDM framework's Path Sequencing Algorithm component determines the visiting order of these waypoints. The chosen sequencing strategy directly affects path efficiency, exploration time, and gas map reconstruction accuracy. To identify the most effective sequencing approach for the WS-GDM framework, four classical algorithms are implemented and evaluated including Nearest Neighbour (NN), TSP with NN initialization (TSP-NN), NN with 2-opt optimization (NN-2opt), and Ant Colony Optimization (ACO). While these algorithms are well known in general path optimization literature, their integration and comparative evaluation within a gas distribution mapping workflow remain unexplored. In particular, the use of the NN-2opt hybrid method for GDM applications has not been reported in prior studies, motivating its inclusion in this work. This section describes the operational principles and implementation details of each algorithm within the WS-GDM framework.

3.4.1 Nearest Neighbour

The Nearest Neighbour (NN) algorithm is a greedy path sequencing strategy that incrementally constructs a route by always selecting the nearest unvisited waypoint from the robot's current position. Beginning at the robot's start location, NN repeatedly computes the Euclidean distance to all remaining coordinates and appends the closest one to the path. This process continues until all waypoints have been visited. Although NN operates with very low computational cost and is suitable for real-time applications, it often results in suboptimal paths because it considers only local decisions without global optimization. Nonetheless, its speed and simplicity make it a widely used baseline for path planning. Table 1 presents the pseudo-code for the NN algorithm.

Table 1 Nearest Neighbour Pseudocode

Nearest Neighbour pseudocode form	
1	**Procedure** Nearest Neighbour Algorithm
2	**Initialize path = [origin]**
3	Unvisited = all points in coords
4	

5	while Unvisited not empty:
6	**Select nearest point p from Unvisited to last(path)**
7	Append p to path
8	Remove p from Unvisited
9	
10	return path

3.4.2 TSP – NN

The TSP-NN algorithm extends the basic NN by treating the waypoint arrangement as a Travelling Salesman Problem (TSP). It first generates a complete path using the NN heuristic, then connects the last waypoint back to the origin, forming a closed loop similar to a TSP tour. This method aims to minimize total travel distance while ensuring that each location is visited exactly once. While not guaranteed to produce the optimal TSP solution, TSP-NN improves path efficiency compared to the basic NN approach, especially in structured environments or repetitive exploration tasks. Table 2 shows the pseudo code form for TSP – NN algorithm.

Table 2 TSP - Nearest Neighbour Pseudocode

TSP - Nearest Neighbour pseudocode form	
1	**Procedure** TSP - Nearest Neighbour Algorithm
2	**Initialize path = [origin]**
3	Unvisited = all points in coords
4	
5	while Unvisited not empty:
6	**Select nearest point p from Unvisited to last(path)**
7	Append p to path
8	Remove p from Unvisited
9	
10	Append origin to close the loop
11	return path

3.4.3 NN – 2 OPT

The NN-2opt algorithm enhances the initial NN path through a 2-Opt local optimization process. After constructing the NN route, the 2-Opt procedure iteratively examines all pairs of edges in the path and swaps each point connections if doing so shortens the total distance. This process continues until no further improvement can be made, resulting in a more globally efficient route. The NN-2opt algorithm strikes a balance between computational cost and path optimality, making it a practical solution for field robots requiring efficient yet adaptive route planning. Notably, this work is the first to couple the NN–2opt hybrid method with Gas Distribution Mapping (GDM), applying the combination specifically to improve waypoint sequencing for gas-mapping tasks. Table 3 shows the pseudo code form for NN – 2opt.

Table 3 NN – 2 Opt Pseudocode

Nearest Neighbour – 2 Opt pseudocode form	
1	**Procedure** Nearest Neighbour – 2 Opt Algorithm

```
    Initialize path = [origin]
    Unvisited = all points in coords

    while Unvisited not empty:
        Select nearest point p from Unvisited to last(path)
        Append p to path
        Remove p from Unvisited
    repeat
        improved = False
        for each pair of indices (i, j) in path:
            new_path = path with segment [i:j] reversed
            if distance(new_path) < distance(path):
                path = new_path
                improved = True
    until not improved

    return path
```

3.4.4 Ant Colony Optimization

The Ant Colony Optimization algorithm is a bio-inspired metaheuristic that simulates the foraging behaviour of ants to find optimal routes. In ACO, multiple artificial "ants" explore possible waypoint sequences, guided by two main components including pheromone trails, which represent accumulated experience of previous successful paths, and heuristic desirability, typically based on the inverse of distance. Over iterations, pheromone levels are updated to reinforce shorter paths while weaker routes gradually evaporate. This iterative process allows ACO to converge toward near-optimal solutions. Although computationally more intensive than NN-based methods, ACO offers superior global optimization performance, especially in complex or dynamic environments. Table 4 shows the pseudo code form for ACO algorithm.

Table 4 ACO Pseudocode

Ant Colony Optimization pseudocode form

```
Procedure Ant Colony Optimization Algorithm
    Initialize pheromone τ on all edges
    for each iteration:
        for each ant k in N:
            Construct path using probability:
                P(i,j) ∝ [τ(i,j)]^a [1 / distance(i,j)]^β
            Evaluate path length
            Update best_path if shorter

        Evaporate pheromone: τ ← (1 - ρ) * τ
        Reinforce pheromone along best paths

    return best_path
```

Each of these path sequencing algorithms is integrated into the WS-GDM framework as alternative configurations, enabling systematic comparison under identical conditions. The waypoints generated by the Waypoint Generator component serve as input to each algorithm, which then computes an optimized visiting sequence. The mobile robot follows this sequence to collect gas measurements, which are subsequently processed by the Gas Distribution Mapping module. By evaluating all four algorithms within the same framework using consistent waypoints and environmental conditions, this study identifies which path sequencing method achieves the optimal balance between exploration efficiency and mapping accuracy for gas distribution applications. Fig. 4 illustrates the comparison process between the studied path sequencing algorithms.

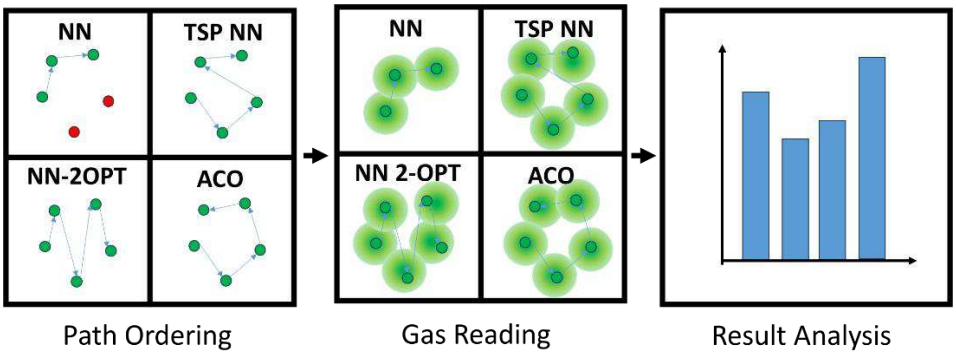

Fig 4. Path sequencing algorithm comparison in WS-GDM

3.5 Ground Truth Gas map, Gas Sampling and Mapping Process

The ground truth gas map represents an idealized and noise-free gas concentration field used for evaluating the robot's gas mapping performance. In gas distribution mapping (GDM) research, such maps provide a reference for comparing reconstructed maps generated by a mobile robot against a known "true" distribution. Since actual gas behaviour is complex and difficult to measure precisely at every location, synthetic ground truth maps are typically generated using computational models that approximate realistic gas diffusion behaviour based on physics-inspired principles.

Common approaches for generating ground truth maps include Gaussian diffusion models, computational fluid dynamics (CFD) simulations, and experimental grid measurements. Among these, the Gaussian diffusion model is the most widely used due to its simplicity and computational efficiency. In this approach, each gas source is modelled as a Gaussian field where concentration decreases with distance from the source, optionally incorporating wall-aware attenuation factors to simulate airflow obstruction caused by physical barriers. This method provides a physically plausible yet computationally lightweight approximation suitable for mobile robot simulations and benchmarking studies. In this work, the Gaussian diffusion model was implemented based on Equation (5), where (x_s, y_s) represents the gas source location, σ is the diffusion spread parameter, and $C(x, y)$ is the gas concentration value at point (x, y).

$$C(x, y) = \exp\left(\frac{(x - x_s)^2 + (y - y_s)^2}{2\sigma^2}\right) \tag{5}$$

In this work, the ground truth generation process begins by loading the arena's occupancy map and its corresponding YAML metadata to retrieve map resolution and origin coordinates. Each pixel corresponds to a real-world coordinate in meters. A distance transform is computed from the free-space

mask to model wall effects on gas propagation. Two gas sources are positioned at the approximate centres of the two enclosed rooms, as indicated by green circles in Fig. 5, simulating realistic gas leak scenarios within confined spaces rather than open areas. For each defined gas source position, a Gaussian diffusion model is applied to simulate gas concentration decay with distance. A wall-decay multiplier attenuates gas intensity near walls, representing airflow obstruction effects. After summing contributions from both sources, the gas field is normalized between 0 and 1 and overlaid on the map background to produce a visually interpretable heatmap. The result is saved as both a PNG image for visualization and a NumPy array for computational analysis during WS-GDM framework evaluation. Fig. 5 illustrates the generation process from the occupancy map to the ground truth gas distribution map based on the Gaussian Diffusion Model, with gas source locations marked by green circles.

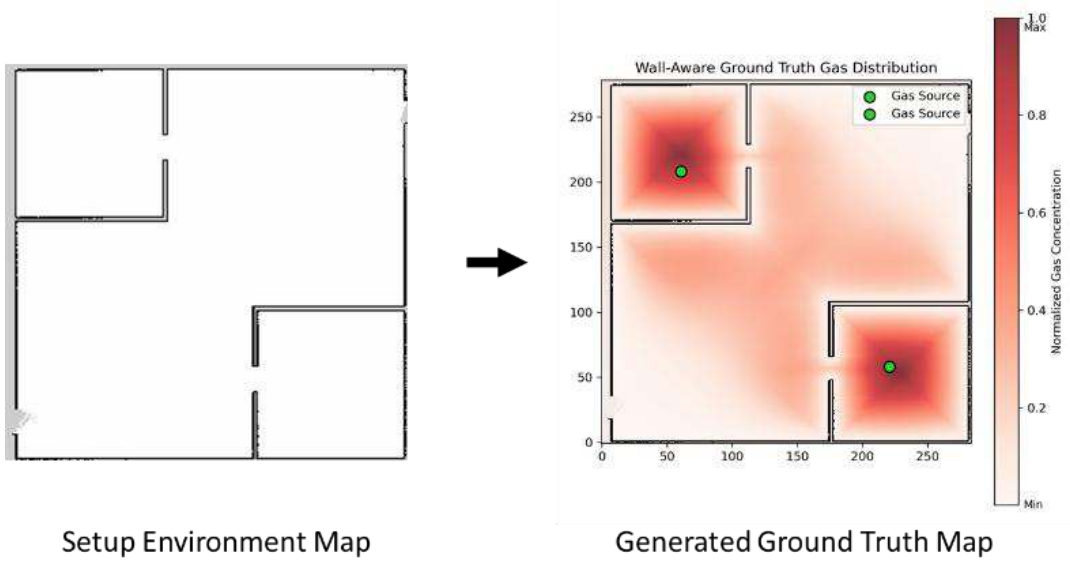

Fig 5. Generated Gas Ground Truth Map

After generating the ground truth gas map, the Gas Distribution Mapping component reconstructs the concentration field by processing measurements collected along the path determined by the Path Sequencing Algorithm. As the mobile robot navigates to each waypoint in the computed sequence, it collects gas concentration measurements at that location. The system records each visited position along with a confidence value reflecting local coverage quality. These measurements are overlaid onto the arena map in real time to progressively build the reconstructed gas distribution.

Each gas measurement is represented as a circular region using a Gaussian spread with a 1-meter diffusion radius, simulating how gas concentration decreases with distance from the measurement point. The diffusion radius of 1 meter is chosen to balance spatial coverage and measurement precision, providing sufficient overlap between adjacent sampling points while avoiding excessive smoothing of concentration gradients. To reconstruct the gas field from sparse robot measurements, the Kernel DM+V method is employed. This approach extrapolates each point measurement across the environment by using a Gaussian kernel that spreads its influence to nearby cells. By accumulating these kernels, the algorithm produces both a distribution map (DM) and a variance map (V), representing the estimated concentration and confidence at each location. The resulting reconstructed gas distribution map is then compared against the ground truth map to evaluate mapping accuracy. This comparison enables assessment of how effectively each path sequencing configuration within the WS-GDM framework samples and reconstructs the gas field, providing the basis for identifying the optimal Path Sequencing Algorithm for the framework.

3.6 Experimental Setup and Evaluation Metrices

The experiments were conducted in a simulated indoor environment to evaluate different configurations of the WS-GDM framework with varying path sequencing algorithms. The environment structure was based on an occupancy grid map, where white areas represent free space and black areas indicate walls or obstacles. A corresponding ground truth gas map was generated using a Gaussian diffusion model to simulate realistic gas spread from multiple sources, as described in the previous subsection. This ground truth map served as the reference for evaluating the accuracy of the framework's reconstructed gas distribution.

The Waypoint Generator component in WS-GDM framework produced optimal sampling locations using adaptive Gaussian K-Means clustering based on predicted gas distribution. Four path sequencing algorithms were implemented as alternative configurations of the Path Sequencing Algorithm component including NN, TSP-NN, NN-2opt, and ACO. Each algorithm produced a different visiting order, affecting the exploration path, travel efficiency, and quality of gas distribution reconstruction. During each simulation run, the mobile robot followed the computed path sequence and collected gas measurements at each waypoint. The system recorded each visited position along with a confidence value reflecting local coverage quality. These measurements were continuously processed by the Gas Distribution Mapping component and overlaid onto the arena map in real time as coloured Gaussian patches, progressively building the reconstructed gas distribution.

Four primary evaluation metrics were used to assess each WS-GDM framework configuration:

1. **Number of Sampling Coordinates:** The total number of waypoints where the robot collected gas measurements. Fewer sampling points indicate more efficient spatial coverage with less data redundancy.
2. **Path Length:** The total distance travelled by the robot to visit all sampling locations. Shorter paths indicate more efficient and compact trajectories, reducing travel time and energy consumption.
3. **Completion Time:** The total time required for the robot to complete the entire sampling sequence, including navigation and data collection. Lower completion times indicate faster and more practical exploration performance.
4. **Gas Mapping Accuracy:** How closely the reconstructed gas distribution matches the ground truth map, measured using Mean Squared Error (MSE) and Pearson correlation coefficient. Higher accuracy indicates better representation of the actual gas concentration field.

All framework configurations were tested under identical conditions, using the same ground truth gas distribution, map resolution, and gas source locations. Each configuration was evaluated five times to ensure repeatability and robustness of the results. Together, these metrics and experimental controls provided a comprehensive evaluation for identifying the optimal path sequencing method within the WS-GDM framework.

4.0 RESULT AND DISSCUSION

4.1 Overview

This section presents the experimental results and comparative analysis of different WS-GDM framework configurations with varying path sequencing algorithms. The evaluation examines four implementations of the Path Sequencing Algorithm component including Nearest Neighbour (NN), Travelling Salesman Problem with Nearest Neighbour initialization (TSP-NN), Nearest Neighbour with 2-opt optimization (NN-2opt), and Ant Colony Optimization (ACO). While all configurations begin from the same starting position, each path sequencing method generates different sampling coordinate sets through the adaptive Waypoint Generator, which responds dynamically to the robot's stopping positions along its path, resulting in distinct waypoint distributions for each framework variant.

The performance analysis is organized into three main aspects which are sampling density and area coverage, path characteristics and completion time, and gas mapping accuracy relative to the ground truth map. Each WS-GDM configuration is evaluated using four quantitative metrics defined in Section 3, including number of sampling points, path length, completion time, and mapping accuracy measures. Through this comprehensive evaluation, the study identifies the optimal path sequencing method for the WS-GDM framework. The following subsections present these results in detail, supported by visual representations of path trajectories and reconstructed gas distribution maps.

4.2 Sampling Density and Coverage Result

This subsection examines the spatial coverage and sampling density achieved by different WS-GDM framework configurations to understand how path sequencing methods affect the completeness of gas distribution mapping. Fig. 6 shows the gas map coverage achieved by each framework variant across five test runs. Coverage is calculated as the percentage of the total 10m × 10m environment area covered by the Kernel DM+V gas distribution reconstruction based on collected measurements. The results indicate that WS-GDM with NN-2opt produced the highest average coverage at 85.54%, with its best performance in Test 3, followed by WS-GDM with NN at 83.92%, TSP-NN at 81.71%, and ACO with the lowest coverage at 79.49%. These coverage differences are influenced by the number of sampling points collected, as shown in Table 5, though the relationship is not strictly proportional due to potential overlap and spatial distribution of measurements. The NN-2opt configuration generated the most sampling points with an average of 47 points, followed by NN with approximately 46 points, TSP-NN with 43 points, and ACO with the fewest at 42 points. The variation in sampling density stems from the unique visiting sequence generated by each path sequencing algorithm. Since the framework's Waypoint Generator responds adaptively to each stopping position, different path sequences lead to different subsequent waypoint selections, ultimately affecting the total coverage achieved by each configuration.

In summary, WS-GDM with NN-2opt achieved approximately 1.92% higher coverage than the NN configuration, 4.70% higher than TSP-NN, and 7.61% higher than ACO. Similarly, the NN configuration outperformed TSP-NN by 2.71% and ACO by 5.58%, while TSP-NN exceeded ACO by 2.79%. These differences correlate with the number of sampling points generated, where NN-2opt collected approximately 2.17% more points than NN, 9.30% more than TSP-NN, and 11.90% more than ACO. This demonstrates that framework configurations employing dense sampling strategies, particularly NN-2opt and NN, achieved substantially higher spatial coverage compared to optimization-focused methods like TSP-NN and ACO. While TSP-NN and ACO reduced the number of waypoints by approximately 8-11% compared to NN-2opt, this efficiency came at the cost of 5-8% reduction in

area coverage. This trade-off highlights a critical consideration for the WS-GDM framework which is maximizing comprehensive spatial coverage through dense sampling versus minimizing travel distance through optimized routing.

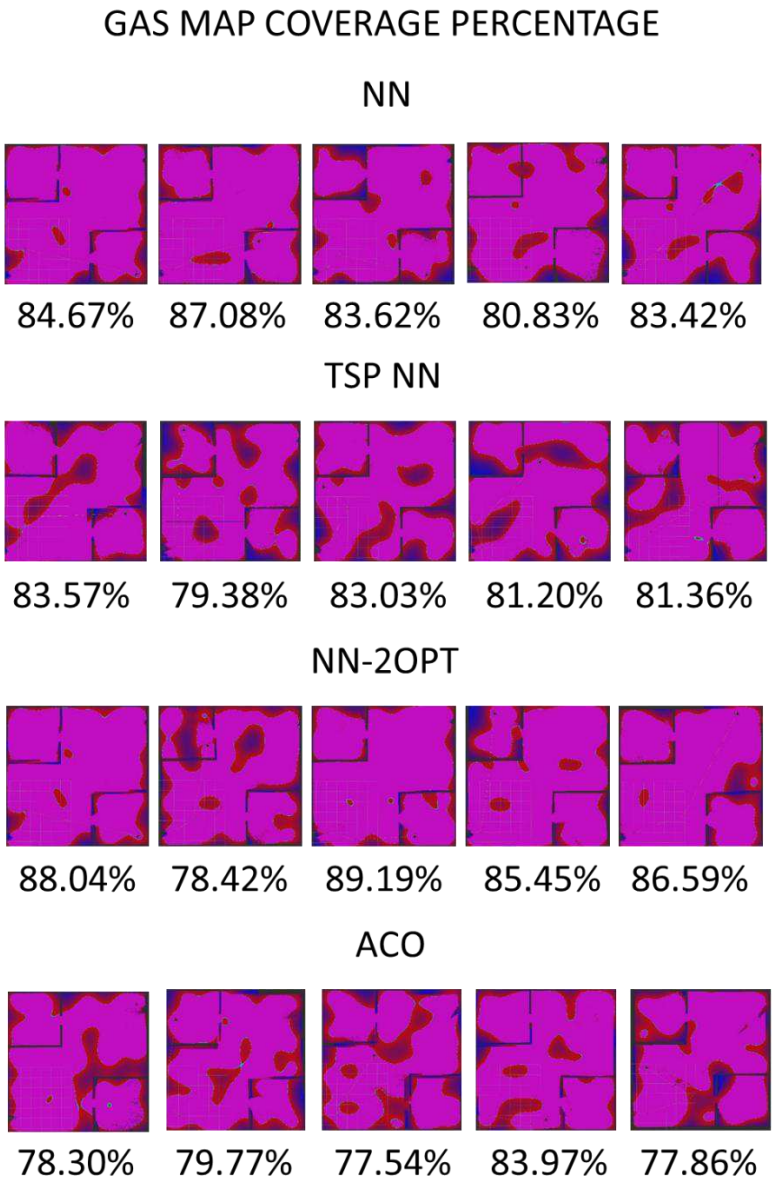

Fig 6. Gas Map Coverage Percentage

Table 5 Number of Sampling point and Average Coverage

Path Sequencing Algorithm	Number of sampling point					Avg No. Point	Avg Coverage (%)
	Test 1	Test 2	Test 3	Test 4	Test 5		
NN	49	48	46	44	44	46.2	83.924
TSP NN	44	42	43	42	44	43	81.708
NN-2OPT	48	41	49	47	48	46.6	85.538
ACO	42	41	39	45	42	41.8	79.488

4.3 Path Visualization and Completion Time Result

The second evaluation aspect examines the path trajectories and completion times resulting from different WS-GDM framework configurations. Fig. 7 illustrates the paths taken by the mobile robot and the cumulative distance travelled to reach all sampling points for each framework variant. The results show that WS-GDM with NN-2opt generated the most efficient path structure, followed by TSP-NN, NN, and ACO configurations. Notably, efficient paths required shorter cumulative distances despite visiting more sampling points, as demonstrated by the NN-2opt, TSP-NN, and NN configurations. In contrast, the WS-GDM with ACO configuration produced a less organized path, resulting in significantly longer cumulative distance even with fewer sampling points to visit.

The path organization and distance travelled strongly influenced completion time, as shown in Table 6. Completion time represents the total mission duration, including travel time between waypoints, waypoint generation through adaptive clustering, and path sequencing computation. WS-GDM with TSP-NN achieved the fastest completion time at 2958.90 seconds, followed by NN-2opt at 3141.36 seconds, NN at 3180.38 seconds, and ACO with the longest completion time at 3204.10 seconds. These completion times strongly correlated with the cumulative distance travelled which TSP-NN covered the shortest distance at 113.40m, followed by NN-2opt at 118.63m, NN at 121.71m, and ACO with the longest distance at 173.34m.

In summary, the TSP-NN configuration completed the mapping task 5.81% faster than NN-2opt, 7.48% faster than NN, and 8.28% faster than ACO, while traveling 4.41% less distance than NN-2opt, 7.34% less than NN, and 52.88% less than ACO. Although the NN-2opt configuration achieved only 1.23% longer completion time than TSP-NN, it collected approximately 9.30% more sampling points, demonstrating both good path efficiency and high sampling density. The most significant finding is the ACO configuration's performance. Despite visiting the fewest points (11.90% fewer than NN-2opt), it travelled 46.12% more distance and required 7.81% more time than NN-2opt due to its poorly organized path structure. This analysis reveals that path organization and routing efficiency have a stronger impact on completion time than the absolute number of sampling points. Well-optimized configurations like WS-GDM with TSP-NN and NN-2opt can visit more locations in less time by minimizing backtracking and unnecessary detours, whereas poorly optimized paths like the ACO configuration result in substantial time and distance penalties regardless of sampling density.

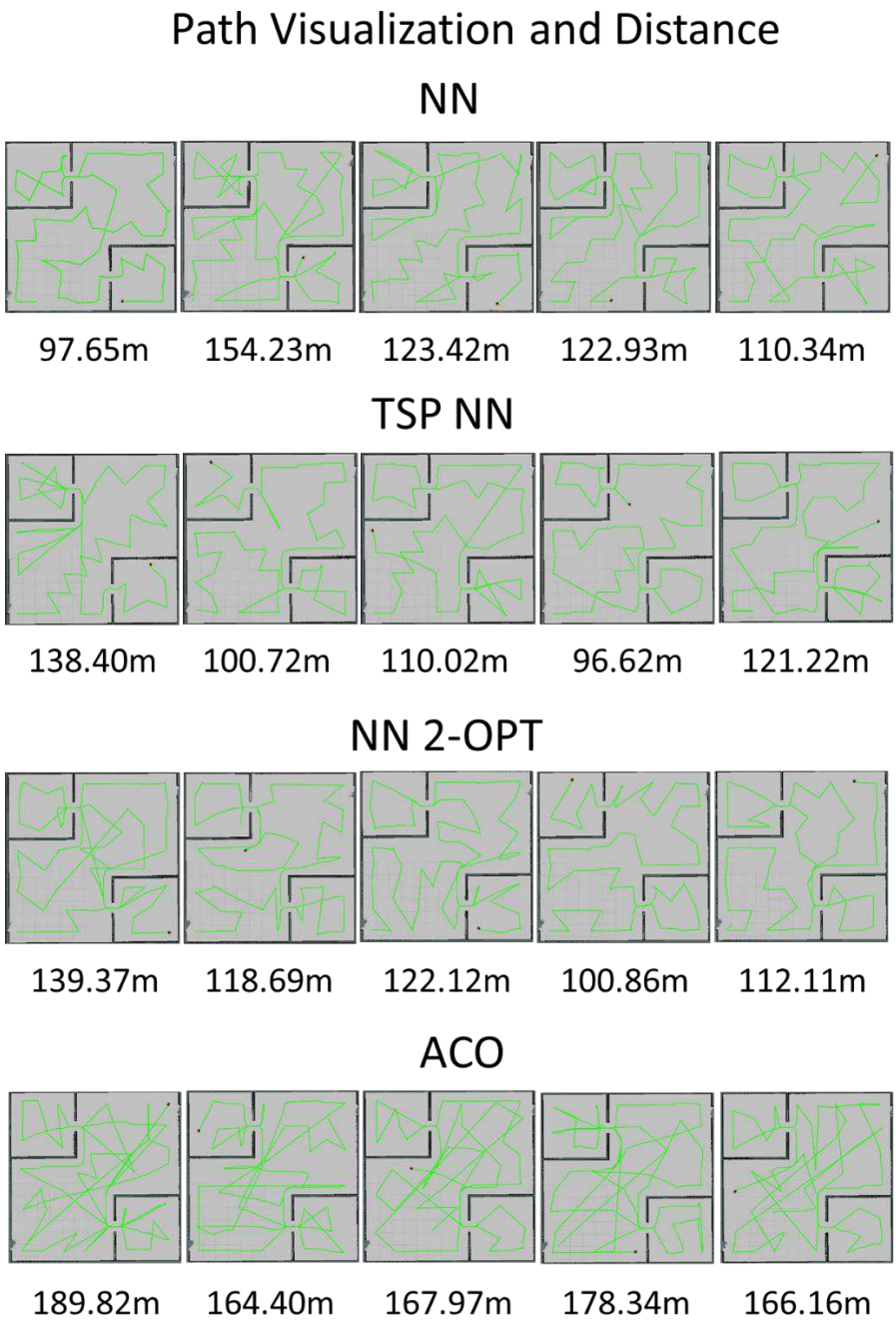

Fig 7. Path Visualization and Cumulative Distance

Table 6 Completion Time and Average Path Distance

Path Sequencing Algorithm	Completion Time (s)					Avg Time (s)	Avg Path Distance (m)
	Test 1	Test 2	Test 3	Test 4	Test 5		
NN	3573.41	3269.68	3120.45	3250.84	2687.53	3180.382	121.714
TSP NN	3949.58	2670.24	2798.31	2479.77	2896.61	2958.902	113.396
NN-2OPT	3863.46	3029.37	3019.24	2670.93	3123.78	3141.356	118.63
ACO	3154.84	2765.84	2664.10	4353.84	3081.89	3204.102	173.338

4.4 Gas Distribution Mapping Accuracy and Gas Source Location

The third evaluation aspect examines the accuracy of gas distribution mapping and gas source localization achieved by different WS-GDM framework configurations compared to the ground truth map. The reconstructed gas maps were compared to the ground truth at a resolution of 0.05m per coordinate location. Fig. 8 presents the mapping accuracy results across all tests. As shown, all framework configurations achieved gas mapping accuracy exceeding 85% when compared to the ground truth map. WS-GDM with NN achieved the highest average accuracy at 89.33%, followed closely by NN-2opt at 89.29%, ACO at 89.16%, and TSP-NN at 89.10%. The difference between the best and worst performing configurations was only 0.26%, indicating that all variants produced similarly accurate gas concentration maps. This high mapping accuracy across all configurations can be attributed to the substantial area coverage achieved, which exceeded 79%, providing sufficient spatial sampling to reconstruct the gas distribution field reliably.

Beyond overall mapping accuracy, the precision of gas source localization was evaluated by comparing the detected source location to the ground truth position, as shown in Fig. 9. The detected source location is identified as the coordinate with the highest reconstructed gas concentration in the Kernel DM+V map. The results reveal varying performance across framework configurations. WS-GDM with ACO exhibited the least consistent performance, maintaining relatively high distance errors ranging from 0.65m to 1.4m across all tests. The NN configuration showed better overall performance but with high variability, including one notably accurate detection in Test 3 at approximately 0.45m but higher errors in other tests. In contrast, TSP-based configurations including TSP-NN and NN-2opt demonstrated more stable source localization, maintaining distance errors between 0.45m and 1.0m throughout all tests. WS-GDM with NN-2opt achieved the most consistent performance with the best average distance error of 0.524m across all tests.

Despite achieving similar overall mapping accuracy above 89%, the spatial pattern of reconstructed gas distribution maps differs significantly across configurations, directly affecting source localization precision. The path pattern strongly influences the resulting gas map pattern which well-organized paths with minimal crossings, such as those generated by NN-2opt, produce more coherent concentration gradients that accurately represent the gas field structure. In contrast, disorganized paths with frequent crossings and backtracking, as observed in ACO, create irregular sampling patterns that distort concentration gradients and obscure the true source location. This explains why NN-2opt, with its optimized 2-opt refinement that eliminates path crossings, achieves superior source localization despite having similar area coverage to other methods. The systematic path structure enables more accurate reconstruction of concentration peaks, leading to precise source identification.

In summary, while gas mapping accuracy showed minimal variation across framework configurations with only 0.26% difference, gas source localization revealed more significant performance distinctions. The NN-2opt configuration's average source localization error was 19.26% lower than NN, 24.64% lower than TSP-NN, and 52.52% lower than ACO. Despite the ACO configuration achieving comparable gas mapping accuracy, its source localization was significantly less accurate, demonstrating 110.88% higher error than NN-2opt. This disparity reveals that high area coverage and gas mapping accuracy do not necessarily guarantee precise source localization. The relationship between metrics shows that path organization plays a critical role which show by WS-GDM with NN-2opt's well-structured path with 85.54% coverage and organized sampling pattern enabled both high mapping accuracy and precise source detection. Conversely, the ACO configuration's disorganized path, despite achieving 79.49% coverage and 89.16% mapping accuracy, resulted in poor source localization due to sub-optimal sampling distribution around the actual source location. This indicates that the Path

Sequencing Algorithm component significantly affects not only efficiency metrics but also the spatial quality of gas distribution reconstruction within the WS-GDM framework, particularly for identifying concentrated emission sources.

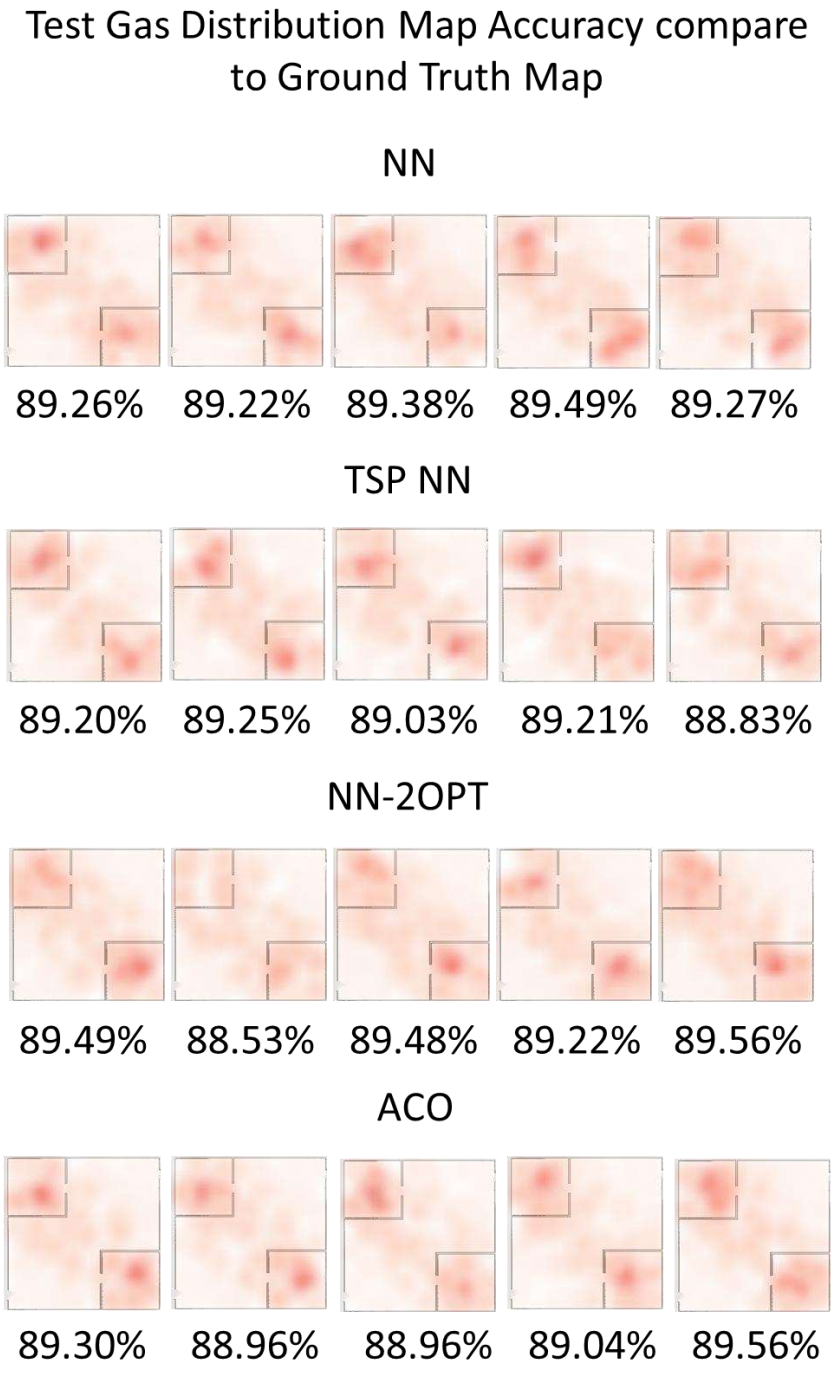

Fig 8. Gas Distribution Map Accuracy Compared to Ground Truth Gas Map

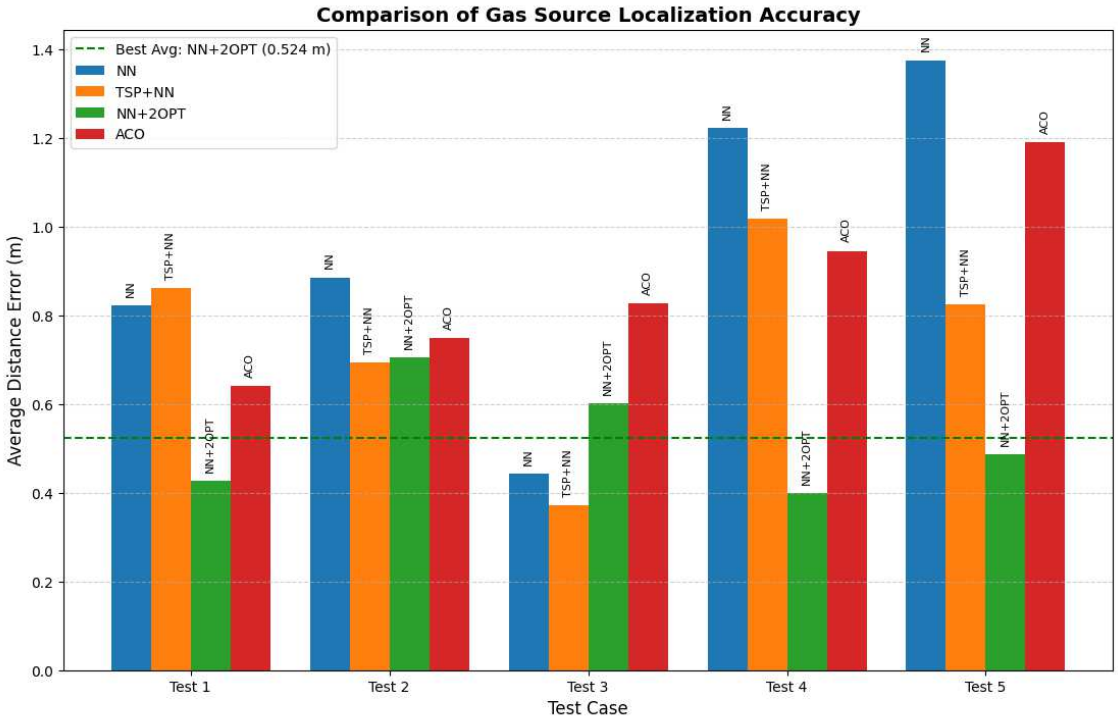

Fig 9. Average Distance Error for all path sequencing algorithm across test

4.5 Summary of Findings

The comparative evaluation of four WS-GDM framework configurations reveals distinct performance characteristics that directly relate to each path sequencing algorithm's underlying operational principles. WS-GDM with NN (Nearest Neighbour) operates on a greedy, locally optimal decision-making approach, always selecting the closest unvisited point. This configuration resulted in high sampling density with an average of 46 points and coverage at 83.92%, leading to good gas mapping accuracy at 89.33%. However, the lack of global path optimization resulted in moderate path efficiency, with completion time 7.48% slower than the TSP-NN configuration despite achieving comparable mapping accuracy. NN's localized decision-making explains its high variability in source localization performance, as the greedy approach does not strategically position sampling points around potential source regions.

WS-GDM with TSP-NN applies the Travelling Salesman Problem formulation with nearest neighbour initialization to achieve global path optimization while ensuring complete waypoint coverage. This configuration produced the most efficient traversal, achieving the shortest completion time at 2958.90s and distance at 113.40m which 5.81% faster and 4.41% shorter than NN-2opt. However, the emphasis on distance minimization resulted in fewer sampling points at 43 points, 8.51% fewer than NN-2opt, and consequently lower area coverage at 81.71%. While gas mapping accuracy remained high at 89.10%, the reduced sampling density led to moderate source localization precision with 0.695m average error, demonstrating that global path optimization alone does not guarantee optimal sensing coverage.

WS-GDM with NN-2opt combines the greedy nearest neighbour initialization with local search optimization through iterative edge swapping by 2-opt. This hybrid configuration achieved the best overall balance across metrics: highest coverage at 85.54%, most sampling points at 47 points, well-organized path structure, and most consistent source localization at 0.524m average error which 19.26%

better than NN and 24.64% better than TSP-NN. The 2-opt refinement eliminated path crossings and reduced unnecessary detours while maintaining high sampling density, resulting in only 6.16% longer completion time than TSP-NN but 4.70% better coverage. This demonstrates that local path refinement can significantly improve both efficiency and sensing quality simultaneously within the WS-GDM framework. The superior performance of NN-2opt can be attributed to its path structure characteristics: the 2-opt refinement produces paths with minimal crossings and systematic coverage patterns, creating more coherent concentration gradients in the reconstructed gas map. This organized sampling pattern enables accurate identification of concentration peaks, leading to precise source localization.

WS-GDM with ACO employs a probabilistic, nature-inspired metaheuristic that iteratively constructs solutions through pheromone-guided exploration. While theoretically capable of finding near-optimal solutions, this configuration's performance was limited by the fewest sampling points at 42 points and poorest path organization, resulting in the longest travel distance at 173.34 which 52.88% longer than TSP-NN and highest completion time at 3204.10s. Despite achieving comparable gas mapping accuracy at 89.16%, only 0.19% lower than NN-2opt, the ACO configuration exhibited the worst source localization performance with 1.105m average error, 110.88% higher than NN-2opt. ACO's disorganized path with frequent backtracking creates irregular sampling patterns that distort concentration gradients, making source identification more difficult despite achieving similar overall mapping accuracy. This suggests that ACO's stochastic exploration mechanism, while effective for pure distance optimization problems, may not adequately prioritize spatial sampling distribution critical for environmental sensing tasks within the WS-GDM framework.

The results reveal that the Path Sequencing Algorithm component significantly influences both operational efficiency and sensing quality in the WS-GDM framework. Configurations prioritizing sampling density, such as NN and NN-2opt, achieved superior coverage and source localization at the cost of slightly longer paths, while distance-optimizing configurations like TSP-NN and ACO reduced travel distance but compromised spatial sampling quality. Notably, WS-GDM with NN-2opt emerged as the most robust configuration, demonstrating that hybrid approaches combining greedy initialization with local optimization can effectively balance the competing objectives of exploration efficiency, area coverage, and mapping accuracy. Based on these findings, NN-2opt is identified as the optimal Path Sequencing Algorithm for the WS-GDM framework, providing superior balance between operational efficiency and mapping fidelity. For specific application requirements, TSP-NN offers the fastest completion time for time-critical missions, while NN provides straightforward implementation with moderate performance across all metrics.

5.0 CONCLUSION

This paper proposed the Waypoint-Sequencing Gas Distribution Mapping (WS-GDM) Framework, an integrated system combining adaptive Gaussian K-Means waypoint generation, classical path sequencing algorithms, and Kernel DM+V gas field reconstruction for autonomous environmental monitoring in completely unknown environments. The framework addresses critical research gaps by systematically integrating adaptive waypoint generation with path sequencing while evaluating their combined impact on operational efficiency and gas mapping accuracy, and by operating in scenarios where both spatial structure and gas distribution are simultaneously unknown to the robot. Through comparative evaluation of four classical path sequencing algorithms including NN, TSP-NN, NN-2opt, and ACO, the study presents the first implementation of NN combined with 2-opt optimization specifically for gas distribution mapping applications. Results demonstrated that WS-GDM with NN-2opt achieved the most robust performance with highest coverage at 85.54% and most accurate source localization at 0.524m average error, while WS-GDM with TSP-NN provided fastest completion at 2958.90s. A significant finding revealed that high area coverage does not guarantee accurate source

localization, as all configurations achieved mapping accuracy above 89% yet source localization errors varied from 0.524m to 1.105m. This demonstrates that path organization and spatial sampling distribution, rather than coverage percentage alone, critically affect source detection precision. Based on comprehensive evaluation, NN-2opt is identified as the optimal path sequencing method for the WS-GDM framework, achieving superior balance between exploration efficiency and sensing quality through its organized path structure with minimal crossings. Future work should validate the framework using physical robots in real-world environments with sensor noise and turbulence, test in outdoor and larger-scale settings, develop adaptive sequencing methods, evaluate multi-source scenarios, and explore multi-robot implementations to enhance practical applicability for autonomous environmental monitoring.

ACKNOWLEDGEMENT

The author would like to acknowledge the support from the Fundamental Research Grant Scheme (FRGS) under a grant number of FRGS/1/2022/TK08/UNIMAP/03/13 from the Ministry of Higher Education Malaysia.

REFERENCES

[1] S. Rangeetha, S. Shimona, K. V. Sneha, and N. R. Subashri, "VR Based Robot Navigation System for Gas Leakage Detection and Surveillance," in *2025 6th International Conference on Data Intelligence and Cognitive Informatics, ICDICI 2025*, Institute of Electrical and Electronics Engineers Inc., 2025, pp. 1857–1863. doi: 10.1109/ICDICI66477.2025.11135174.

[2] V. P. Tran, A. G. Perera, M. A. Garratt, K. Kasmarik, and S. G. Anavatti, "Active Sensing Strategy: Multi-Modal, Multi-Robot Source Localization and Mapping in Real-World Settings with Fixed One-Way Switching," Jul. 2024, [Online]. Available: http://arxiv.org/abs/2407.01308

[3] S. Yadav, S. Shukla, R. Tiwari, and M. P. Yadav, "Path planning for mobile robots with waypoint management using a hybrid nature inspired optimization algorithm," *Cluster Comput*, vol. 28, no. 6, Oct. 2025, doi: 10.1007/s10586-025-05111-8.

[4] D. Selvaraj and S. K. Senthil, "Intelligent Robotic Path Planning Based on SPIDI-Lion Optimization Algorithm Using Deep Spectral LSTM-Gated Convolution Neural Network," *Cognit Comput*, vol. 17, no. 4, Aug. 2025, doi: 10.1007/s12559-025-10464-8.

[5] A. Merei, H. Mcheick, A. Ghaddar, and D. Rebaine, "A Survey on Obstacle Detection and Avoidance Methods for UAVs," Mar. 01, 2025, *Multidisciplinary Digital Publishing Institute (MDPI)*. doi: 10.3390/drones9030203.

[6] B. Moon *et al.*, "IA-TIGRIS: An Incremental and Adaptive Sampling-Based Planner for Online Informative Path Planning," Sep. 2025, [Online]. Available: http://arxiv.org/abs/2502.15961

[7] K. Sharma, V. P. Singh, A. Ebrahimnejad, and D. Chakraborty, "A hybrid clustering and greedy routing approach to solve a two-level location allocation and a static dial-a-ride problem," *OPSEARCH*, 2025, doi: 10.1007/s12597-025-01002-z.

[8] W. Kuang, H. W. Ho, and Y. Zhou, "CPP-DIP: Multi-objective Coverage Path Planning for MAVs in Dispersed and Irregular Plantations," May 2025, [Online]. Available: http://arxiv.org/abs/2505.04989

[9] E. Alanzi and M. E. B. Menai, "Solving the traveling salesman problem with machine learning: a review of recent advances and challenges," *Artif Intell Rev*, vol. 58, no. 9, Sep. 2025, doi: 10.1007/s10462-025-11267-x.

[10] R. Alkhalifa, F. Alkhomayes, B. Almazroua, D. Alhaidan, M. Alothman, and J. Almuhaidib, "A Comparative Review of Parallel Exact, Heuristic, Metaheuristic, and Hybrid Optimization Techniques for the Traveling Salesman Problem," May 2025, [Online]. Available: http://arxiv.org/abs/2505.18278

[11] M. Goel, J. Singh, and A. Kumar Bairwa, “Performance Evaluation of Heuristic and Meta-Heuristic Algorithms on Large-Scale Travelling Salesman Problem Instances,” *IEEE Access*, vol. 13, pp. 156988–157010, 2025, doi: 10.1109/ACCESS.2025.3606531.

[12] H. Li and J. Wang, “A Collaborative Neurodynamic Optimization Algorithm Based on Boltzmann Machines and 2-Opt Heuristic for Solving the Traveling Salesman Problem,” in *17th International Conference on Advanced Computational Intelligence, ICACI 2025*, Institute of Electrical and Electronics Engineers Inc., 2025, pp. 1–8. doi: 10.1109/ICACI65340.2025.11096345.

[13] H. Zhao, Z. Ma, L. Liu, Y. Wang, Z. Zhang, and H. Liu, “Optimized Path Planning for Logistics Robots Using Ant Colony Algorithm under Multiple Constraints,” in *2025 8th International Conference on Advanced Algorithms and Control Engineering, ICAACE 2025*, Institute of Electrical and Electronics Engineers Inc., 2025, pp. 464–467. doi: 10.1109/ICAACE65325.2025.11019278.

[14] S. Ashur, N. M. Amato, and S. Har-Peled, “Edge Nearest Neighbor in Sampling-Based Motion Planning,” Jun. 2025, [Online]. Available: http://arxiv.org/abs/2506.13753

[15] G. Li, C. Liu, L. Wu, and W. Xiao, “A mixing algorithm of ACO and ABC for solving path planning of mobile robot,” *Appl Soft Comput*, vol. 148, Nov. 2023, doi: 10.1016/j.asoc.2023.110868.

[16] A. Abdukodirov and J. Benndorf, “Recent Developments in Path Planning for Unmanned Ground Vehicles in Underground Mining Environment,” Jun. 01, 2025, *Multidisciplinary Digital Publishing Institute (MDPI)*. doi: 10.3390/mining5020033.

[17] H. Liu, J. Luo, L. Zhang, H. Yu, X. Liu, and S. Wang, “Research on Traversal Path Planning and Collaborative Scheduling for Corn Harvesting and Transportation in Hilly Areas Based on Dijkstra’s Algorithm and Improved Harris Hawk Optimization,” *Agriculture (Switzerland)*, vol. 15, no. 3, Feb. 2025, doi: 10.3390/agriculture15030233.

[18] L. Xu, M. Xi, R. Gao, Z. Ye, and Z. He, “Dynamic path planning of UAV with least inflection point based on adaptive neighborhood A* algorithm and multi-strategy fusion,” *Sci Rep*, vol. 15, no. 1, Dec. 2025, doi: 10.1038/s41598-025-92406-w.

[19] M. Kulich, J. Kubalík, and L. Přeučil, “An integrated approach to goal selection in mobile robot exploration,” *Sensors (Switzerland)*, vol. 19, no. 6, Mar. 2019, doi: 10.3390/s19061400.

[20] J. Janos, V. Vonasek, and R. Penicka, “Multi-Goal Path Planning Using Multiple Random Trees,” *IEEE Robot Autom Lett*, vol. 6, no. 2, pp. 4201–4208, Apr. 2021, doi: 10.1109/LRA.2021.3068679.

[21] Y. Lu and E. Plaku, “Combining Machine Learning and Sampling-Based Search for Multi-Goal Motion Planning with Dynamics,” Mar. 2025, [Online]. Available: http://arxiv.org/abs/2503.20530

[22] P. Khumla and K. Sarawan, “Efficient Route Planning in Northeast Thailand Using a Random Shuffle Enhanced 2-opt Algorithm-optRS Improve 2-opt Route Planning Northeast region of Thailand Traveling Salesman Problem Corresponding Author,” 2025. [Online]. Available: http://creativecommons.org/licenses/by-sa/4.0/

[23] S. Banerjee and A. C. Mondal, “An intelligence technique for route distance minimization to store and marketize the crop using computational optimization algorithms,” *Sci Rep*, vol. 15, no. 1, Dec. 2025, doi: 10.1038/s41598-025-14263-x.

[24] Y. Lu and C. Da, “Global and local path planning of robots combining ACO and dynamic window algorithm,” *Sci Rep*, vol. 15, no. 1, Dec. 2025, doi: 10.1038/s41598-025-93571-8.

[25] T. Zhou and W. Wei, “Mobile robot path planning based on an improved ACO algorithm and path optimization,” *Multimed Tools Appl*, vol. 84, no. 12, pp. 10899–10922, Apr. 2025, doi: 10.1007/s11042-024-19370-x.

[26] A. Gongora, J. Monroy, F. Rahbar, C. Ercolani, J. Gonzalez-Jimenez, and A. Martinoli, “Information-Driven Gas Distribution Mapping for Autonomous Mobile Robots,” *Sensors*, vol. 23, no. 12, Jun. 2023, doi: 10.3390/s23125387.

[27] I. Kulbaka, A. Dutta, O. P. Kreidl, L. Bölöni, and S. Roy, “GDM-Net: Gas Distribution Mapping with a Mobile Robot Using Deep Reinforcement Learning and Gaussian Process Regression,” in *IEEE International Conference on Intelligent Robots and Systems*, Institute of Electrical and Electronics Engineers Inc., 2024, pp. 4511–4518. doi: 10.1109/IROS58592.2024.10802502.

[28] N. P. Winkler, P. P. Neumann, E. Schaffernicht, and A. J. Lilienthal, “Gas Distribution Mapping With Radius-Based, Bi-directional Graph Neural Networks (RABI-GNN),” in *ISOEN 2024 - International Symposium on Olfaction and Electronic Nose, Proceedings*, Institute of Electrical and Electronics Engineers Inc., 2024. doi: 10.1109/ISOEN61239.2024.10556309.

[29] C. Ercolani, L. Tang, and A. Martinoli, “GaSLAM: An Algorithm for Simultaneous Gas Source Localization and Gas Distribution Mapping in 3D,” in *IEEE International Conference on Intelligent Robots and Systems*, Institute of Electrical and Electronics Engineers Inc., 2022, pp. 333–340. doi: 10.1109/IROS47612.2022.9981976.

[30] I. K. Waarum, A. van Hove, T. R. Krogstad, K. O. Ellefsen, and A. E. A. Blomberg, “Mixtures of Gaussian processes for robotic environmental monitoring of emission sources,” *Environ Monit Assess*, vol. 197, no. 6, Jun. 2025, doi: 10.1007/s10661-025-14059-6.

[31] A. J. Lilienthal, M. Reggente, M. Trincavelli, J. L. Blanco, and J. Gonzalez, “A statistical approach to gas distribution modelling with mobile robots—the Kernel DM+V algorithm,” in Proc. IEEE/RSJ Int. Conf. Intell. Robots Syst. (IROS), Oct. 2009, pp. 570–576.

[32] M. M. Zainal et al., "Spider-Tree: Ordered Rooted Tree-Based Entrance Organizer for Unknown Area Exploration," 2025 9th International Conference on Man-Machine Systems (ICoMMS), Malacca, Malaysia, 2025, pp. 273-278, doi: 10.1109/ICoMMS66553.2025.11200310.